Noise in grown alumina tunnelling barriers

1992 J. Phys.: Condens. Matter 4 8053

(http://iopscience.iop.org/0953-8984/4/40/019)

J. Phys.: Condens. Matter 4 (1992) 8053–8072. Printed in the UK

Noise in grown alumina tunnelling barriers

A M Speakman and C J Adkins
Cavendish Laboratory, Madingley Road, Cambridge CB3 0HE, UK

Received 28 May 1992, in final form 21 July 1992

Abstract. Conductance noise was measured in tunnel junctions with alumina barriers grown by plasma oxidation or thermal oxidation in atmospheres containing different amounts of water. Noise measurements were made in the frequency range 7 Hz–70 kHz, under biases −1 V to +1 V, and at temperatures 1 K to 4.2 K. In junctions with barriers grown under dry conditions, shot noise dominated at all frequencies. In junctions with barriers grown in the presence of water, noise power at low frequencies was four orders of magnitude larger than shot noise; it had an approximately $1/f$ frequency variation and a strong bias dependence, but was temperature independent below 4.2 K. We show that the results are not quantitatively consistent with models involving modulation of the tunnelling barrier. We develop a new model, based on switching of resonant channels, that is able to explain the levels of noise observed.

1. Introduction

Grown aluminium oxide is the classic tunnelling barrier because of the ease with which continuous layers with low leakage (non-tunnelling) current are formed, at thicknesses suitable for tunnel barriers. Oxide films are grown on aluminium either by exposure to atmosphere (thermal oxidation) or by exposure to an oxygen glow discharge (plasma oxidation). The growth rate decreases with oxide thickness, so the process is self-limiting. Several studies have been reported which compare the conductance spectra of thermal and plasma grown oxide barriers, prepared in atmospheres of varying humidity (Bowser and Weinberg 1977, Dragoset *et al* 1982). Inelastic electron tunnelling spectra confirm the accepted picture of an amorphous alumina (Al_2O_3) barrier with OH^- surface contaminants. The IET spectra published in the above reports become noticeably noisier as the degree of water contamination increases. However, no direct noise measurements have previously been reported for this type of tunnel barrier.

In this study, electrical noise (fluctations in conductance) was measured in tunnel junctions with alumina barriers grown by plasma oxidation or thermal oxidation in atmospheres containing different amounts of water. Conductance measurements were made on the same junctions. A valid interpretation of the noise data must be consistent with that of the conductance spectra.

2. Sample preparation

In each preparation, three junctions of areas 100 μm × 100 μm, 100 μm × 150 μm and 200 μm × 200 μm were prepared simultaneously on a single substrate. Base

0953-8984/92/408053+20$04.50

aluminium electrodes were deposited by vacuum evaporation, and an oxide layer was grown upon them to form the tunnel barrier. Oxidation times and conditions were chosen to give sample resistances of about 2 kΩ.

Four different oxidation techniques were used.

(i) Plasma oxidation by exposure to a 100 mA, 1 kV discharge in 0.15 mbar of oxygen for one hour in the evaporator.

The vacuum chamber was pre-cleaned by a glow discharge so that when the discharge was turned on again for plasma oxidation, the glow was pale grey/blue, showing that the oxygen discharge was clean and dry. IET spectra of completed junctions (section 4) showed that plasma oxides had much less hydrocarbon and OH contamination than thermal oxides (types (ii) to (iv)).

(ii) Exposure to room air for 1 hour.

(iii) Exposure to moist room air for 1 hour—over a beaker of water at room temperature.

(iv) Exposure to water vapour for several seconds—vapour from water at 50 °C was allowed to condense visibly on the substrate.

Some of the clean junctions (oxide type i) were doped with water or organic impurities by exposure of the clean oxide surface to moist room air or formic acid vapour. After preparation of the barrier, the vacuum chamber was pumped down again, and lead or aluminium top electrodes were deposited across the base electrodes.

On removal from the vacuum chamber, the set of three junctions on one substrate was immediately slotted into an edge connector mounted on an insert. This was dipped into liquid helium for measurements at 4.2 K, or cooled in a pumped helium cryostat for measurements down to 1 K. The insert was wired to enable switching between the three junctions without removal from the cryostat. Over a period of several days in helium, there was no ageing of the junction resistance, and all conductance and noise measurements were repeatable.

3. Measurement techniques

3.1. Conductance measurements

Differential conductance $\mathrm{d}I/\mathrm{d}V$ and conductance derivative $\mathrm{d}^2I/\mathrm{d}V^2$ were measured as a function of bias at 4.2 K. The measurement system is described fully by Speakman (1991). It uses operational amplifiers to maintain a voltage bias and small modulation voltage across a four-terminal tunnel junction in a bridge circuit. The first and second harmonic current components, proportional to $\mathrm{d}I/\mathrm{d}V$ and $\mathrm{d}^2I/\mathrm{d}V^2$, are detected by a lock-in amplifier across the bridge. The voltage source and lock-in amplifier are under computer control, and spectra are recorded automatically. The $\mathrm{d}I/\mathrm{d}V$ versus bias curve gives an indication of the tunnel barrier height, width and asymmetry, and peaks in the $\mathrm{d}^2I/\mathrm{d}V^2$ spectrum show any dominant energies lost by tunnelling electrons to phonons or vibrational modes of impurity molecules.

3.2. Noise measurements

The junction was biased with a DC current I_b, and the noise voltage across it was measured differentially using an EG&G PAR model 5301 lock-in amplifier in noise mode. In this mode, the phase sensitive detector output is rectified and smoothed,

and the 5301 gives a reading of the input voltage noise v_n (in V $Hz^{-1/2}$) at the reference frequency f in a bandwidth $1/\tau$ where τ is the lock-in time constant. The noise measurement option is available for $\tau = 300$ ms (1 Hz equivalent noise bandwidth) and $\tau = 30$ ms (10 Hz ENBW), and the smoothing time, which is the time necessary to make a measurement, is preset at approximately 5 min for $\tau = 300$ ms and 30 s for $\tau = 30$ ms.

Background noise was measured at zero bias current for junctions with aluminium top electrodes, and at a small bias current for junctions with lead top electrodes, to move the junction voltage away from the lead superconducting gap region around zero bias. Samples of resistance 400 Ω to 4 kΩ had background noise levels within the range 10–20 nV $Hz^{-1/2}$ at all measurement frequencies. This is insignificant compared with sample $1/f$ noise at low frequencies (figure 3(*a*)), but background subtraction was necessary at higher frequencies when shot noise was dominant (figure 3(*b*)).

At each bias current I_b, and frequency f, the noise generated in the junction, $v_n(f, I_b)$, was calculated by subtracting the background noise across the junction $v_b(f, 0)$ from the measured noise $v_m(f, I_b)$ using

$$v_n^2 = v_m^2 - v_b^2.$$

4. Conductance results

For junctions with lead top electrodes, the structure in dI/dV near zero bias due to the superconducting gap of lead was the same strength for oxides prepared using any of the four oxidation techniques. This shows that the dominant transport process at low bias was electron tunnelling in all junctions.

Conductance curves for barriers prepared using different oxidation techniques are shown in figure 1 for junctions with lead top electrodes and in figure 2 for junctions with aluminium top electrodes. In these and subsequent data, positive bias means that the base electrode is biased positively with respect to the top electrode. All curves are asymmetric, the conductance being greater on the positive bias side. The asymmetry of the conductance curve is a measure of the asymmetry of the tunnel barrier. In the trapezoidal barrier model of Brinkman *et al* (1970), the barrier height ϕ_2 at the top electrode is greater than the height ϕ_1 at the base electrode. It has been suggested that the large asymmetry for junctions with lead top electrodes is due to hydroxyl groups attached to the surface of the oxide film (Dragoset *et al* 1982). IET spectra showed that more OH was present in thermal oxides, which explains the greater asymmetry of the conductance curves of thermal oxides compared to that of a dry plasma oxide (figure 1). The asymmetry is not so large in junctions with aluminium top electrodes. Aluminium has a smaller atomic size than lead, and is more reactive, so that the top electrode metal penetrates (or may decompose) any OH on the oxide surface (Sleigh *et al* 1989). For the same reason, doping by exposure to moist air or formic acid vapour after oxidation did not affect the conductance of junctions with aluminium top electrodes. When the top electrode was lead, doping increased the junction resistance and the asymmetry of the conductance curve, and also gave rise to peaks in the d^2I/dV^2 spectrum as described below.

Increased curvature of the conductance curve for barriers grown under wetter conditions occurs in junctions with either lead or aluminium top electrodes and so

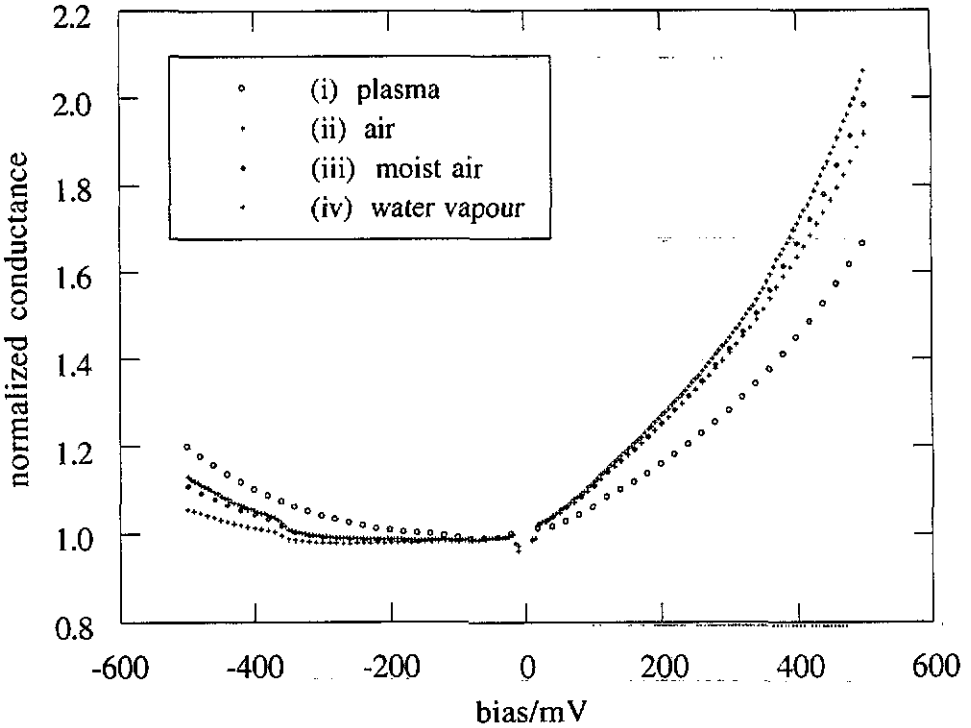

Figure 1. Differential conductance of junctions with Pb top electrodes, normalized to the value at −20 mV bias. The values of dV/dI at 20 mV were: (i) 3.7 kΩ, (ii) 2.0 kΩ, (iii) 15.7 kΩ, (iv) 20 kΩ. The roman numerals refer to the oxide type.

depends on the 'bulk' barrier material rather than on any surface molecules. The increased curvature could result from an increased inelastic contribution to the tunnel current: If tunnelling electrons excite atomic vibrations with a wide energy spread within the barrier, the number of inelastic tunnelling channels increases with increasing bias, so this adds to the curvature of the conductance curve. It is proposed later that inelastic tunnelling in barriers grown under wetter conditions gives rise to the $1/f$ noise observed in these junctions (section 6).

As expected, second-derivative (d^2I/dV^2) spectra had alumina phonon peaks, and when the top electrode was lead there were also peaks due to the excitation of surface hydroxide and hydrocarbon molecules. However, for oxide barriers grown under wetter conditions, inelastic electron tunnelling peaks became 'washed out'. In these junctions, tunnelling electrons lose energy to atomic vibrations with a wide energy spread within the barrier, so that threshold energies for excitation of surface molecules or the alumina phonon are less well resolved.

5. Noise results

Noise in clean junctions was essentially shot noise only over the whole range of frequency and bias; but excess noise was found when barriers were grown in the presence of water. Figure 3 shows the variation of voltage noise v_n with bias at 4.2 K for an oxide barrier grown in moist air with an aluminium top electrode. These results illustrate most of the features of the noise measured in all types of junction. At high frequencies and low bias, v_n is mainly shot noise. This is shown in figure 4, where

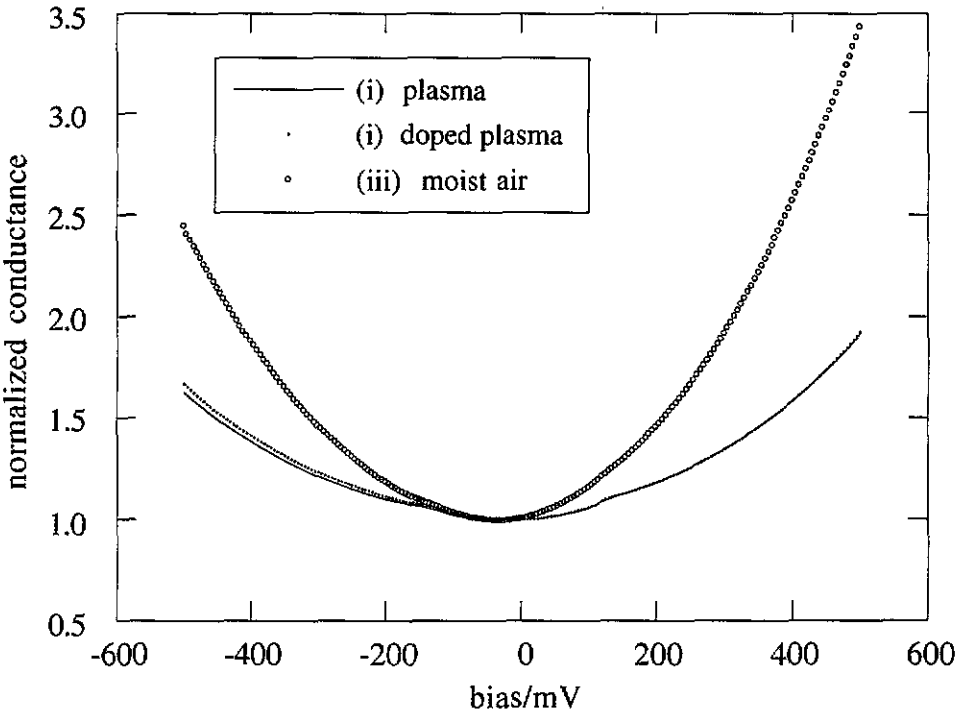

Figure 2. Differential conductance of junctions with Al top electrodes, normalized at zero bias. The values of dV/dI at zero bias were: (i) 360 Ω (undoped), (ii) 740 Ω (doped), (iii) 1.3 kΩ. The roman numerals refer to the oxide type.

the results are plotted as current noise, v_n/Z_s, as calculated from the high-frequency data of figure 3. Here, Z_s is the AC junction impedance given by

$$Z_s(\omega, V) = |(dI/dV) + j\omega C_s|^{-1}$$

where C_s is the junction capacitance. The calculated shot noise, $i_n = \sqrt{2eI_b}$, is shown in figure 4(*b*).

Shot noise is a fundamental and irreducible form of current noise in tunnel junctions, but the junctions had varying amounts of additional noise with an approximately $1/f$ frequency variation. In the following, this excess noise is analysed in terms of a fluctuating tunnel conductance which gives rise to a noise voltage when a steady current passes through the junction.

5.1. Noise viewed as fluctuations of conductance

In section 6 we shall consider a model in which the noise is taken to originate in fluctuations of junction conductance. Here we show how equivalent conductance noise is calculated from measured voltage noise.

Under current bias I_b, time variation of DC junction conductance,

$$G_s(V, t) = G_s(V) + g(V, t)$$

gives rise to a varying junction voltage

$$V(t) = V_0 + v(t)$$

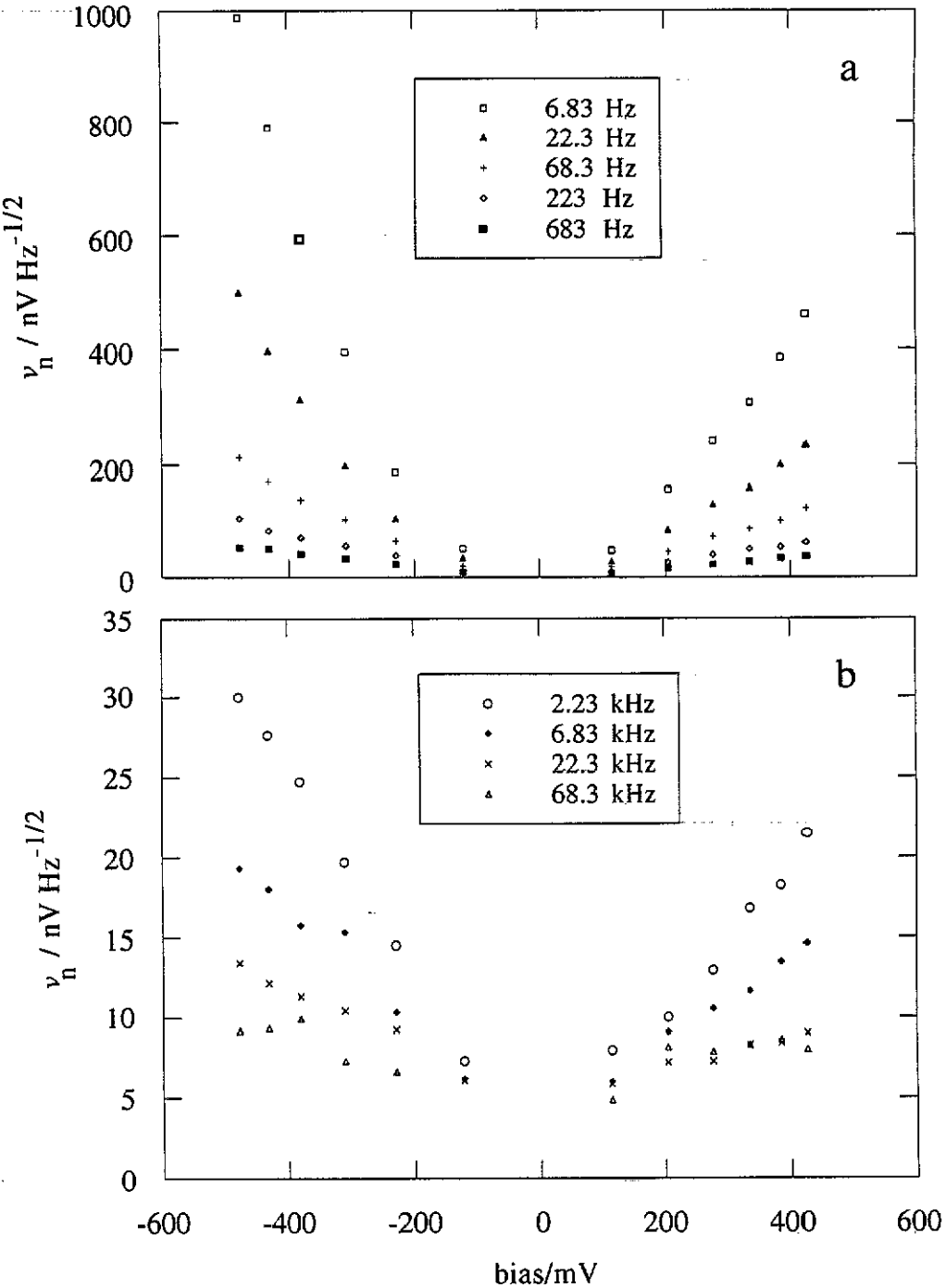

Figure 3. Voltage noise at 4.2 K (after background subtraction) for an oxide of type iii with an Al top electrode. For this junction, dV/dI (0 mV) = 1.3 kΩ, C_s = 0.6 nF.

where

$$I_b = G_s(V,t)V(t) + C_s\,dV(t)/dt = [G_s(V) + g(V,t)][V_0 + v(t)] + C_s\,dV(t)/dt$$

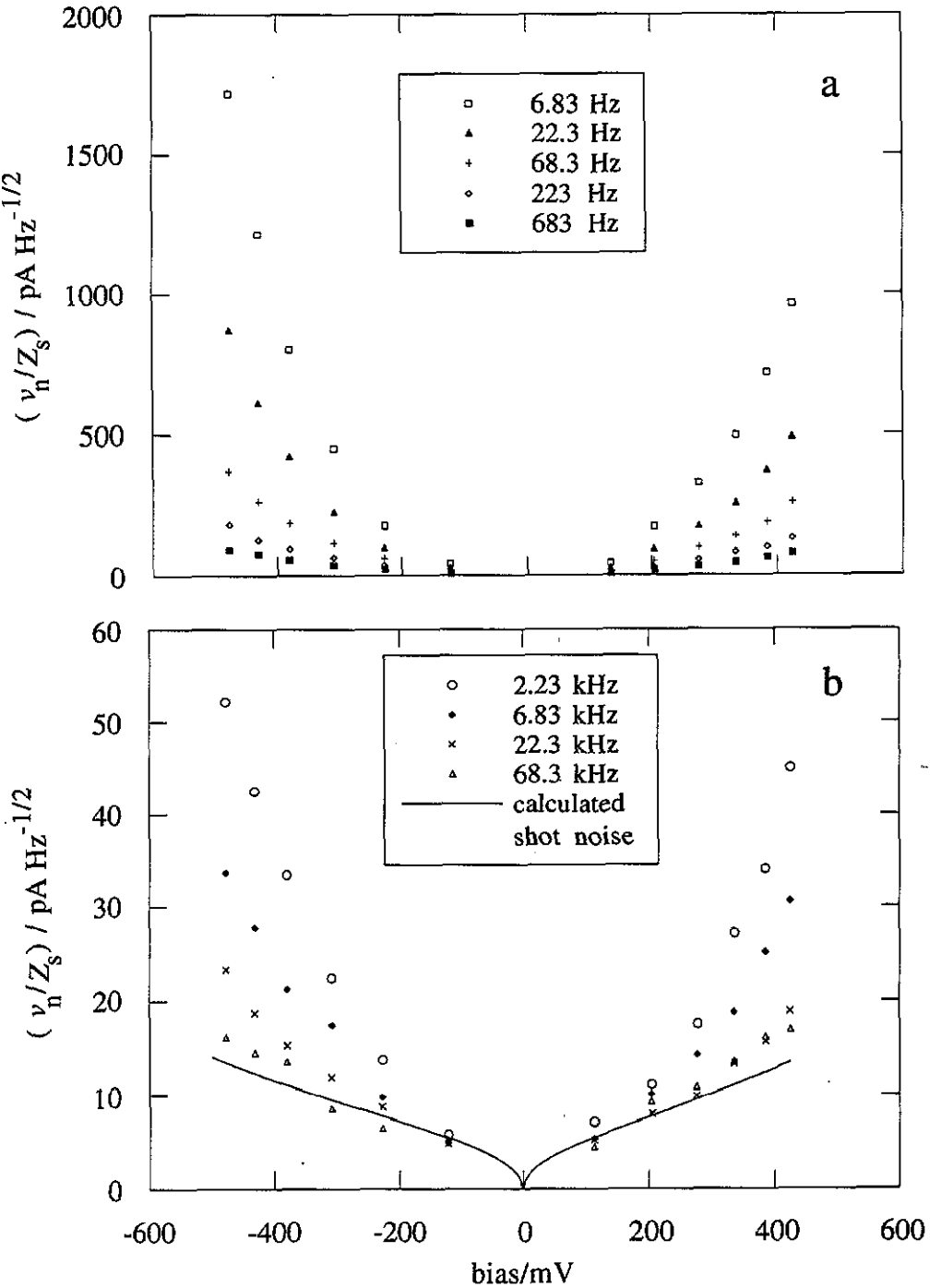

Figure 4. The results of figure 3 plotted as current noise. The curve in (b) shows the calculated shot noise. Shot noise is negligible at the lower frequencies.

$$\approx G_s(V_0)V_0 + [G_s(V_0) + V_0\,\mathrm{d}G_s/\mathrm{d}V]\,v(t) + C_s\,\mathrm{d}v(t)/\mathrm{d}t + V_0 g(V_0, t)$$

$$= G_s(V_0)V_0 + (\mathrm{d}I/\mathrm{d}V)v(t) + C_s\,\mathrm{d}v(t)/\mathrm{d}t + V_0 g(V_0, t).$$

Taking the Fourier transform, $0 = (\mathrm{d}I/\mathrm{d}V)v_\omega + \mathrm{j}\omega C_s v_\omega + V_0 g_\omega$, so

$$g_n/|\mathrm{d}I/\mathrm{d}V + \mathrm{j}\omega C_s| = v_n/V_0$$

gives the conductance noise g_n (Ω^{-1} $\mathrm{Hz}^{-1/2}$) in terms of the measured voltage noise v_n (V $\mathrm{Hz}^{-1/2}$). The fractional conductance noise is

$$g_n/G_s = (|\mathrm{d}I/\mathrm{d}V + \mathrm{j}\omega C_s|/G_s)v_n/V_0 = v_n/Z_s I_b. \tag{1}$$

Figure 5 shows the results of this calculation for the junction of figure 3.

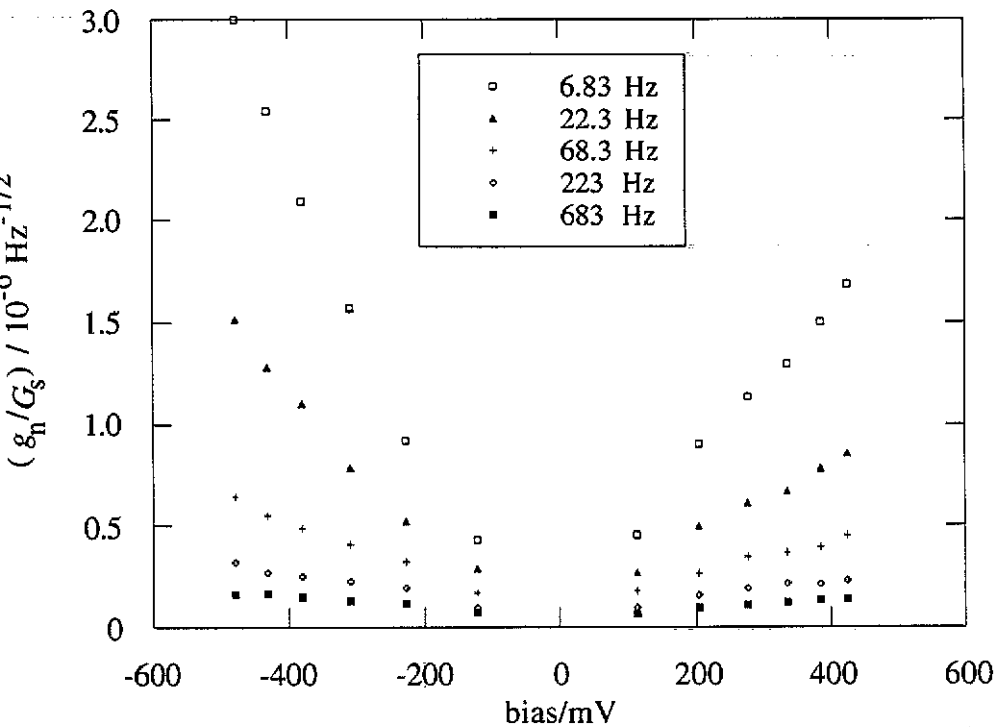

Figure 5. The results of figure 3 plotted as fractional conductance noise, calculated using equation (1).

5.2. Characteristics of the noise

5.2.1. Dependence on sample preparation. The fractional conductance noise g_n/G_s, increased from i to iv in the oxidation methods listed in section 2. Noise in the clean junctions (oxide type i) was close to shot noise level over the whole range of frequency and bias. In figure 5 (oxide type iii), g_n/G_s is an order of magnitude larger than that measured for type ii oxides, but a factor of 3 less than measurements on type iv oxides. The noise level g_n/G_s and its frequency and bias variation depended only on the sample oxidation method, not on the top electrode metal (aluminium or lead). Doping clean junctions with organic molecules or water after oxidation did not give rise to any extra $1/f$ noise in junctions with aluminium top electrodes (and did not affect the junction conductance or IET spectra). The conductance of clean

junctions with lead top electrodes was affected by doping, but still the noise remained closer to that of undoped clean junctions than that of junctions with barriers grown in air.

The noise in these junctions is thus determined by the method of oxidation rather than by the top electrode metal, or by any contamination of the oxide surface.

5.2.2. Area dependence. Within the sets of junctions of different areas produced simultaneously, the noise power g_n^2 scaled with the junction area A, rather than with the length of junction edges $\sqrt{A}$. The noise is therefore a property of the junction area rather than its edges.

5.2.3. Frequency variation. The frequency variation of g_n^2 is not adequately described as a simple $1/f$ dependence. The measurements show varying trends about $1/f$ behaviour, and are most conveniently displayed on a plot of $(v_n/Z_s)\sqrt{f}$ versus f (figure 6). The small variations were reproducible for repeated measurements on the same junction, but occurred at different frequencies and biases for different junctions. The increase of $(v_n/Z_s)\sqrt{f}$ at high frequency occurs because v_n is mainly shot noise at high frequencies, so that v_n/Z_s is frequency-independent shot noise current.

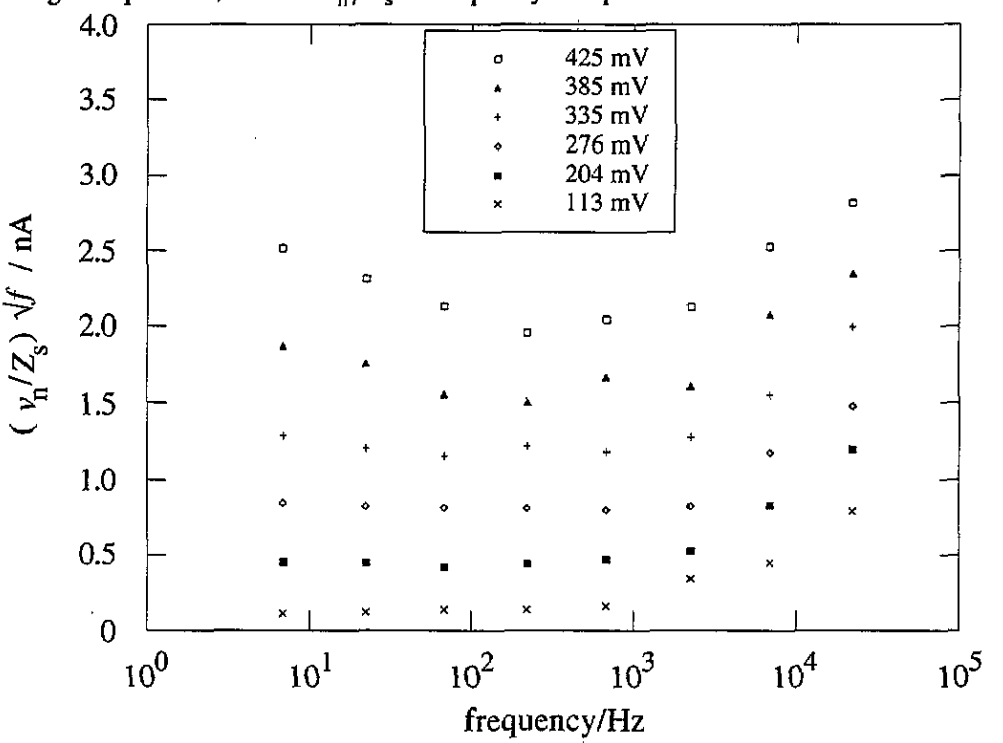

Figure 6. Frequency variation of current noise for the junction of figure 3, plotted to show deviations from $\sqrt{f}$ dependence.

5.2.4. Bias variation. When $1/f$ noise was dominant, the conductance noise g_n increased strongly with bias. This implies that the bias current used to measure g_n, itself excites the noise. For junctions with lead top electrodes, the voltage noise v_n was polarity dependent due to the asymmetry of the conductance curve, dI/dV versus

bias, but the conductance noise curve was approximately symmetric. The conductance noise is thus driven by the bias current, and the voltage noise is the result of the steady bias current passing through the noisy conductance. Noise increased smoothly with bias and the g_n/G_s versus bias curves (figure 5) can be fitted by a low order polynomial.

5.2.5. Temperature variation. The bias variation of the noise was investigated only at 4.2 K, but some samples were cooled in the cryostat, and background noise and noise at 0.5 V bias were measured over the whole frequency range 7 Hz to 70 kHz, at several different temperatures between 4.2 K and 1 K. Within the limits of experimental error, the voltage noise v_n and hence the conductance noise g_n did not vary with temperature in this range.

6. Models for the $1/f$ noise

6.1. Introduction

Fluctuations which have spectral densities varying approximately as $1/f$ over a large frequency range have been observed in a wide variety of dissimilar physical systems, from the loudness of a piece of classical music to the flow of traffic on Japanese motorways. In electronic devices, $1/f$ noise has been explained in terms of an ensemble of microscopic fluctuators with a broad distribution of fluctuation rates (Dutta and Horn 1981). Each fluctuator has a Lorentzian noise spectrum centred on its characteristic fluctuation frequency and summation over an appropriate distribution of characteristic frequencies gives rise to $1/f$ noise. Evidence for this origin of $1/f$ noise has been provided by noise measurements on very-small-area tunnel junctions at low temperature and low bias when only a small number of fluctuators is active (Rogers and Buhrman 1984). The noise spectrum is then resolved into a number of Lorentzian lines which merge into a broad $1/f$ spectrum as the number of contributing fluctuators is increased by increasing the temperature or the junction area.

In order that the noise increases with decreasing frequency, the distribution of characteristic fluctuation frequencies must extend down to the lowest measurement frequency. Low-frequency $1/f$ noise implies the existence of slow fluctuators. In the theory of Rogers and Buhrman, the fluctuators are *electron traps* in the tunnel barrier (Nb_2O_5) which cause barrier height fluctuations, and thus conductance fluctuations, as electrons are captured and released. However, this model is appropriate only at low bias ($\leqslant 20$ mV in their experiments), when it is possible for traps to have energies between the two electrode Fermi energies when empty but below both Fermi energies when occupied. The energy shift is due to lattice distortion caused by interaction between the trapped charge and nearby ions. Electron release thus requires either thermal activation or ionic tunnelling, and the release time is slow enough to account for the low characteristic frequencies of the traps. In the present experiments, noise above the background and shot noise level was observed only at biases of 100 mV or more. Slow electronic release times are not possible for states in the barrier at these energies since the electron does not require activation to tunnel out into states in the positive electrode, and the coupling with electrode states will be similar to that responsible for tunnelling across the barrier, which results in transition times less

than 1 ps (Schäfer and Adkins 1991). The low-frequency noise cannot therefore be the result of charge trapping in the barrier.

Fluctuations in the barrier charge distribution could also occur through *ionic motion* and this can have characteristic frequencies as low as the lowest measurement frequency. Atomic motions with a wide range of excitation energies and relaxation times are necessary to explain the low-temperature properties of structurally disordered materials. In these materials, ions are not constrained to their positions in a crystal lattice, but can hop between neighbouring energy minima. The two-level system model (Phillips 1987) proposes that an atom or a group of atoms moves in a two-well potential. At low temperatures, a quantum mechanical description is necessary and tunnelling of the atom from one minimum to the other gives rise to the very small energy splittings needed if the states are to be observed in thermal experiments at 1 K and below. Kozub (1984) used this model to derive an expression for the low-frequency noise in a tunnel junction with an amorphous barrier material. However, he assumed that the two-level systems were in thermal equilibrium, phonons supplying the small 'tunnel-splitting' energy, and this gives a conductance noise which increases linearly with temperature, but is bias independent. This is not consistent with the temperature independence and strong bias dependence observed here. The temperature independence shows that the noise-causing transitions are not thermally excited at the temperatures of these experiments. Also, the noise was not the result of Joule heating, since the noise level did not correspond to the junction resistance.

The observation of IET spectra shows that tunnelling electrons exchange energy with ions in the barrier. Ionic transitions with long relaxation times could similarly be excited by inelastically tunnelling electrons. In the model developed below, ions interact with tunnelling electrons, and so move between neighbouring potential minima. These motions cause fluctuations in the barrier potential profile and hence in the *elastic* tunnel current. The frequency, temperature and bias variations of the noise are consistent with this model.

Noise increased with increasing presence of water during oxide barrier growth, so the mobile ions probably come from water. One possibility is a rotating O–H dipole moment due to the movement of a proton between equivalent positions on the end of an Al–O–H bond. A similar model, involving rotation of the OH group about an SiO bond within the amorphous matrix, was used to explain low-temperature properties of vitreous silica containing OH impurity (Phillips 1981), and reorientation of surface OH has been seen in tunnel junctions (Konkin and Adler 1980). However, tunnelling electrons do not interact with surface OH in junctions with aluminium top electrodes—the presence of $1/f$ noise but absence of an IET molecular spectrum for junctions with aluminium top electrodes shows that the noise sources are slowly fluctuating dipoles *within* the barrier, while the IET excitations are transitions with fixed excitation energies of surface molecules. Alternatively, the moving ions could be interstitial protons. Protons are the smallest and most mobile ions, and there will be sites of varying energy available between the larger O ions of the oxide. These excitations will have the wide spread in energy and transition rate necessary to explain the $1/f$ noise and the smoothly varying inelastic contribution to the conductance curves.

6.2. Two-well model

The fluctuators are assumed to be ions moving between neighbouring potential minima. The main features of the system of mobile ions can be discussed using

a model where each fluctuator is represented by a particle moving in a two-well potential (figure 7). In the quantum mechanical description of an ion moving in such a potential (Phillips 1987), the wavefunctions of the two lowest energy states spread across both wells, and their energy difference and asymmetry, and transitions from one state to the other, depend on tunnelling through the potential barrier between the wells. If phonons supply the energy difference E_i for the tunnelling transitions, then the relaxation rate is temperature dependent, and integration of the noise over a distribution of relaxation rates would give a temperature-dependent result. To account for the bias dependence and temperature independence of the noise observed here, it is necessary that transitions require electron excitation.

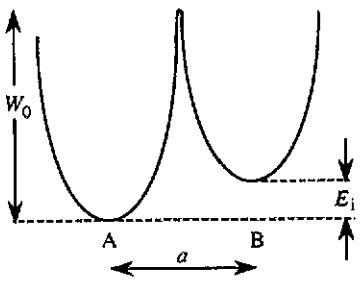

Figure 7. Two-well model.

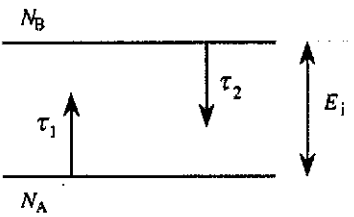

Figure 8. Relaxation times.

6.3. Telegraph noise

The occupancy of well A of a two-well system alternates between 0 and 1 with characteristic times τ_1 and τ_2, where τ_1, τ_2 are the relaxation times for the transitions A $\rightarrow$ B and B $\rightarrow$ A (figure 8). This is telegraph noise with unit pulse height, and it has a Lorentzian power spectrum.

Consider N identical two-well systems. If at time t, N_A are in well A, and N_B in well B, then N_A, N_B satisfy

$$dN_A/dt = N_B/\tau_2 - N_A/\tau_1 \qquad N_A + N_B = N.$$

Combining these two equations,

$$dN_A/dt = -(N_A - N_A^0)/\tau_{eff} \qquad dN_B/dt = -(N_B - N_B^0)/\tau_{eff} \quad (2)$$

where

$$\frac{1}{\tau_{eff}} = \frac{1}{\tau_1} + \frac{1}{\tau_2} \qquad N_A^0 = N\frac{\tau_1}{\tau_1 + \tau_2} \qquad N_B^0 = N\frac{\tau_2}{\tau_1 + \tau_2}. \quad (3)$$

From the differential equation (2), it can be shown (e.g. Van der Ziel 1986) that fluctuations in $(N_A - N_A^0)$ have a Lorentzian power spectrum. The mean square fluctuation per unit frequency f $(= \omega/2\pi)$ is

$$|\Delta N_A(f)|^2 = 4\overline{(N_A - N_A^0)^2}\tau_{eff}/(1 + \omega^2\tau_{eff}^2)$$

where

$$\overline{(N_A - N_A^0)^2} = N\tau_1\tau_2/(\tau_1 + \tau_2)^2. \tag{4}$$

Equation (4) is the binomial variance $Np(1-p)$ with $p = \tau_1/(\tau_1 + \tau_2)$, since N_A follows a binomial probability distribution with maximum value N and mean value $N_A^0 = Np$. The contribution to the power spectrum from a single fluctuator is

$$|\Delta N_A(f)|^2/N = [4\tau_1\tau_2/(\tau_1 + \tau_2)^2]\,\tau_{eff}/(1 + \omega^2\tau_{eff}^2). \tag{5}$$

According to (3), the noise frequency τ_{eff}^{-1} is the sum of the rates τ_1^{-1} and τ_2^{-1}, so for low-frequency noise, both the transition up in energy and the transition down in energy must be slow. This will be the case if both transitions require excitation by an electron.

The conductance noise power per unit frequency due to a single fluctuator is obtained by multiplying the occupation number noise (5) by the square of the conductance fluctuation ΔG due to an individual transition.

$$(g_n/G_s)^2 = (\Delta G/G_s)^2[4\tau_1\tau_2/(\tau_1 + \tau_2)^2]\,\tau_{eff}/(1 + \omega^2\tau_{eff}^2). \tag{6}$$

The fluctuation size ΔG is discussed in section 6.6.

6.4. Distribution of relaxation times

The total conductance noise is given by (6) summed over all two-well systems. As shown below, a $1/f$ noise spectrum can be generated from this summation if the distribution of characteristic times τ_{eff} is proportional to τ_{eff}^{-1}. The $1/f$ spectrum extends over the frequency range $(2\pi\tau_{max})^{-1}$ to $(2\pi\tau_{min})^{-1}$ when the range of the τ_{eff} distribution is $\tau_{min} \leqslant \tau_{eff} \leqslant \tau_{max}$.

Since the relaxation time τ_1 depends on excitation by a tunnelling electron,

$$e/\tau_1 = I_{inel}(A \rightarrow B) \tag{7}$$

where $I_{inel}(A \rightarrow B)$ is the inelastic electron current involving ionic transitions from well A to well B. An equation similar to (7) holds for the transition time τ_2, if excitation by an electron is also needed for the reverse transition.

A transition mechanism which could lead to the required τ_{eff}^{-1} distribution of relaxation times is one in which the ion is excited by a tunnelling electron from the ground state to a higher level in well A, then tunnels to well B. For example, if the potential wells (figure 7) are parabolic ($V = \frac{1}{2}M\omega_0^2x^2$), the ionic wavefunctions are proportional to $\exp(-M\omega_0x^2/2\hbar)$, so that the overlap between states centred on opposite wells is proportional to $\exp(-M\omega_0a^2/4\hbar) \simeq \exp(-2(W_0 - E_j/2)/\hbar\omega_0)$. The ionic tunnelling rate, and hence the transition rates τ_1^{-1} and τ_2^{-1}, are then proportional to the square of this exponential overlap.

$$\tau_{eff}^{-1} \propto \exp(-4W_0/\hbar\omega_0).$$

A uniform distribution of the inter-well barrier strength $w = W_0/\hbar\omega_0$ then satisfies the requirement of a τ_{eff}^{-1} distribution of relaxation times:

$$dN/d\tau_{eff} = (dN/dw)\,dw/d\tau_{eff} = (dN/dw)/4\tau_{eff} \propto 1/\tau_{eff}.$$

For a range of relaxation times $\tau_{min} \leqslant \tau_{eff} \leqslant \tau_{max}$, the normalized distribution is

$$D(\tau_{eff}) = (1/N)\,dN/d\tau_{eff} = 1/\tau_{eff}\ln(\tau_{max}/\tau_{min}). \tag{8}$$

Experimentally, $1/f$ noise was observed in the range of frequency f from $40/2\pi$ Hz to about $20/2\pi$ kHz, so $\tau_{max}^{-1} < 40\ s^{-1}$ and $\tau_{min}^{-1} > 2 \times 10^4\ s^{-1}$. The magnitudes of the rates enter the final expression for the noise only through the normalization factor $\ln(\tau_{max}/\tau_{min})$.

6.5. Summation over all fluctuators

Summing (6) over all fluctuating two-well systems, the total noise is

$$\left(\frac{g_n}{G_s}\right)^2 = \int\int \frac{dN}{dE_i} D(\tau_{eff}) \left(\frac{\Delta G}{G_s}\right)^2 \frac{4\tau_1\tau_2}{(\tau_1+\tau_2)^2} \frac{\tau_{eff}}{(1+\omega^2\tau_{eff}^2)} d\tau_{eff}\, dE_i. \tag{9}$$

Here, the distribution in excitation energy dN/dE_i of the two-well systems is assumed to be approximately independent of the relaxation time distribution $D(\tau_{eff})$. The factor $\tau_1\tau_2/(\tau_1+\tau_2)^2$ decreases from $\frac{1}{4}(\tau_1 \approx \tau_2)$ for $E_i \ll eV$, to zero $(\tau_1 = \infty)$ for $E_i > eV$, so

$$\int \frac{dN}{dE_i} \frac{\tau_1\tau_2}{(\tau_1+\tau_2)^2} dE_i = \frac{1}{4} N_a(V) \tag{10}$$

where $N_a(V)$ is the effective number of active fluctuators at bias V.

Integrating (9), using (8) and (10) leads to

$$(g_n/G_s)^2 = (\Delta G/G_s)^2 (N_a(V)/4f \ln(\tau_{max}/\tau_{min})) \tag{11}$$

in the range $(2\pi\tau_{max})^{-1} < f < (2\pi\tau_{min})^{-1}$. The inverse frequency variation thus arises from integration over a relaxation time distribution proportional to τ_{eff}^{-1}. Variations about $1/f$ behaviour come from deviations from a smooth τ_{eff}^{-1} distribution. The number of active fluctuators $N_a(V)$ increases with bias as long as eV is less than the energy range of the distribution dN/dE_i.

6.6. The contribution from individual fluctuators

In the following, a lower limit for ΔG, the fluctuation size due to an individual fluctuator, is calculated from experimental noise results. We then compare this limit with values obtained from microscopic models. It is shown that the fluctuation size calculated from a simple dipole model is too small, but ΔG from a model involving resonant tunnelling channels is compatible with experiment.

The value of the product $N_a(\Delta G)^2$ can be calculated from noise measurements using (11), so that an estimated upper limit for N_a leads to a minimum fluctuation size ΔG. Rearranging (11),

$$(\Delta G/G_s)^2 = (g_n/G_s)^2 4f \ln(\tau_{max}/\tau_{min})/N_a(V). \tag{12}$$

A reasonable upper limit for N_a is when the fluctuators are 1 nm apart. For a barrier of area $(100\ \mu m)^2$ and thickness 2 nm,

$$N_a < 10^{27} m^{-3} \times [100\ \mu m]^2 \times 2\,nm = 2 \times 10^{10}.$$

Using values quoted in section 6.4, $\ln(\tau_{max}/\tau_{min}) \geqslant 6$, and the maximum measured noise for type iv oxides (0.5 V bias, $f = 6.83$ Hz) was $(g_n/G_s)^2_{max} = 10^{-10} Hz^{-1}$. Substituting these values in (12) gives

$$\Delta G/G_s > 10^{-9}. \tag{13}$$

Consideration of the inelastic current gives an alternative lower limit for ΔG. The inelastic current due to transitions of one two-well system is $I_1 = 2e/(\tau_1 + \tau_2)$, and summing this over all systems,

$$I_{\text{inel}} = \int\int \mathrm{D}(\tau_{\text{eff}}) \frac{\mathrm{d}N}{\mathrm{d}E_i} \frac{2e}{\tau_1 + \tau_2} \mathrm{d}\tau_{\text{eff}} \, \mathrm{d}E_i = \frac{N_a(V)}{4 \ln(\tau_{\max}/\tau_{\min})} \frac{2e}{\tau_{\min}}. \tag{14}$$

Combining (12) and (14),

$$(\Delta G/G_s)^2 = (g_n/G_s)^2 \, 2ef/I_{\text{inel}} \tau_{\min}$$

and since $I_{\text{inel}} < I_{\text{total}} \approx 250\,\mu\text{A}$ at 0.5 V bias,

$$\Delta G/G_s > 10^{-10}.$$

In this case (13) is therefore the experimental lower limit for ΔG.

6.7. Dipole fluctuators

The simplest model for a fluctuator is a fluctuating electric dipole moment. Motion of a singly charged ion between potential minima, distance a apart, is a change ea in dipole moment. The dipole potential adds to the barrier potential profile and so changes the tunnelling conductance of the junction. Following Kozub (1984), the fractional change in conductance due to a perturbation W is given by

$$\Delta G/G_s \simeq \alpha d \overline{W}/U_0$$

where α is the tunnelling decay rate $\sqrt{2mU_0/\hbar^2}$, d is the barrier thickness, U_0 is the barrier height and $\overline{W}$ is the interaction averaged over the barrier volume Ad. The size of this interaction is affected by image dipoles in the metal electrodes, and so depends on the position and orientation of the fluctuating dipole in the barrier. Also, the dipole interaction is odd under inversion and so integration over the barrier will give zero unless there is some asymmetry (an asymmetric barrier due to intrinsic field or voltage bias, or the dipole being nearer one electrode than the other). However, taking the range of the interaction to be the barrier thickness d, and its average size to be a dipole potential at separation d,

$$\overline{W} = (d^2/A)e^2a/4\pi\epsilon_0\epsilon_r d^2 \qquad \Delta G/G_s = (\alpha d/U_0)e^2a/4\pi\epsilon_0\epsilon_r A. \tag{15}$$

With $\alpha d = 10$, $U_0 = 1$ eV, $a = 0.1$ nm, $\epsilon_r = 8$ and $A = (100\ \mu\text{m})^2$, this gives

$$\Delta G/G_s \approx 10^{-11}$$

which is two orders of magnitude smaller than the minimum estimate (13) from experiment.

We may ask whether the first-order perturbation theory we have used is valid. The condition for validity of first-order perturbation theory with a dipole interaction is

$$(\alpha d/U_0)e^2a/4\pi\epsilon_0\epsilon_r d^2 \ll 1$$

(Kozub 1984). This expression is equal to 0.05 for the above parameters, so (15) should be valid.

In noise experiments on tunnel junctions where the junction area was sufficiently small that one could measure the noise spectrum of an individual fluctuator, several authors have observed fluctuations of larger amplitude than expected. Savo *et al* (1987) measured noise in the critical current of Nb–Al_2O_3–Nb Josephson junctions, at biases of the order of 1 μV when electron trapping is possible. The effective trap area, calculated by assuming that the trapping process locally reduces the critical current to zero, was up to 10^{-10} m^2. The expected area for a single trapped charge (Rogers and Buhrman 1985) is

$$A\,\Delta G/G_s \simeq (\alpha d/U_0)e^2\lambda/4\pi\epsilon_0\epsilon_r$$

(compare (15)) where λ is a length several times d in magnitude. This area is of the order 10^{-17} m^2 for an alumina barrier. Farmer *et al* (1987) suggested that large conductance fluctuations (of effective area 10^{-15} m^2 to 10^{-13} m^2) at high bias in MOS tunnel diodes were the result of simultaneous emptying and filling of interacting electron traps in the barrier. They noted that the fluctuation rates were 'many orders of magnitude too low to be the rate for electron tunnelling', and proposed that the collective fluctuations were slow because all the electrons had to be trapped or released simultaneously. However, electron trapping does not occur in tunnel barriers where both electrodes are metal, as any potential electron traps are coupled too strongly to electrode states (section 6.1). The above mechanism applies only to MOS tunnel diodes where the density of states in the semiconducting electrode is many orders of magnitude smaller than that in a metal.

6.8. Resonant tunnelling fluctuators

A different way in which a single ionic fluctuator can produce a *large* effect is if the mobile ion has an associated electronic state through which resonant tunnelling can take place such that the resonant channel is turned on and off by the ionic motion. A simple calculation shows that such a mechanism easily satisfies the criterion of equation (13): direct tunnelling varies as $\exp(-2\alpha d)$, but resonant tunnelling is proportional to $\exp(-\alpha d)$ for a resonant state in the middle of the barrier. If the opening of a resonant channel increases the conductance by a factor $\exp(\alpha d)$ over an area of atomic dimensions, a^2,

$$\Delta G/G_s = (a^2/A)e^{\alpha d} = 10^{-12}e^{10} = 2\times 10^{-8}$$

which is much larger than the minimum required by the experimental data (equation (13)). A more detailed calculation based on this model is outlined below.

When a resonant channel is switched by motion of an ion in the barrier, the corresponding conductance fluctuation is $\Delta G = \Delta I/V$, where ΔI is the current carried by the resonant state. This is given by

$$\Delta I = (e/\hbar)\Gamma_L\Gamma_R/(\Gamma_L + \Gamma_R)$$

(see, for example, Wolf 1985). Γ_L, Γ_R are decay widths to the left and right electrodes, and $\Gamma_L \propto \exp(-2\alpha z)$, $\Gamma_R \propto \exp(-2\alpha(d-z))$ for a state distance z from

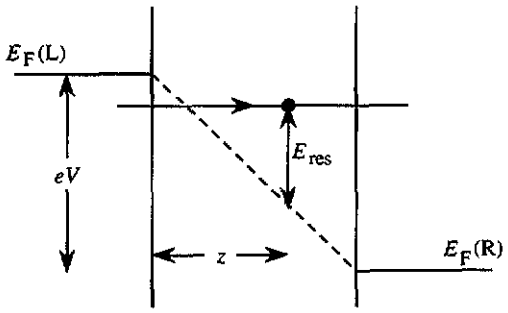

Figure 9. Resonant tunnelling.

the left electrode (figure 9), so ΔI is biggest for states in the middle of the barrier. Then $\Gamma_L = \Gamma_R = \Gamma$ and

$$\Delta I = e\Gamma/2\hbar \propto e^{-\alpha d}. \tag{16}$$

Payne (1986) calculated the resonant tunnelling current via a state in a one-dimensional square well in the middle of the barrier. In that calculation, a one-dimensional density of electrode states was used and this only counts tunnelling perpendicular to the electrode interface. The tunnelling decay rate α varies with $k_{\|}$, the component of electron wavevector parallel to the interface, according to

$$\Delta E = (\hbar^2/2m)(\alpha^2 - k_{\|}^2)$$

where ΔE is the energy depth of the resonant level, measured from the top of the barrier. For a given energy, the decay rate increases with increase of $k_{\|}$, and since tunnelling is proportional to $\exp(-\alpha d)$, the range of contributing $k_{\|}$ values is $\Delta(k_{\|}^2) \approx 2\alpha/d$ and the number of contributing $k_{\|}$ values for electrode area A is $(A/4\pi^2)2\pi\alpha/d$. Multiplying Payne's result by this number gives

$$\Delta I = \frac{e}{\hbar}\frac{4A\alpha^2}{\pi k d}\frac{\hbar^2\alpha^2/2m}{(1+\alpha a/2)}\frac{\hbar^2 k_r^2/2m}{V_0}\frac{\hbar^2 k^2/2m}{U_0}e^{-\alpha(d-a)}$$

where the square well, representing the resonant state, has depth V_0 and width a. U_0 is the barrier height and the wavevectors k and k_r in the electrode and in the well are given by

$$U_0 = (\hbar^2/2m)(\alpha^2 + k^2) \qquad V_0 = (\hbar^2/2m)(\alpha^2 + k_r^2).$$

A similar calculation for a three-dimensional square well of diameter a in the middle of the barrier results in

$$\Delta I = \frac{e}{\hbar}\frac{8}{kd}\frac{\hbar^2\alpha^2/2m}{(1+\alpha a/2)}\frac{\hbar^2 k_r^2/2m}{V_0}\frac{\hbar^2 k^2/2m}{U_0}e^{-\alpha(d-a)}.$$

For $V_0 = U_0 = 1$ eV, $\alpha^2 = k^2 = k_r^2$ and $\alpha d = 10$, this gives $\Delta I = 10^{-9}$ A. For a 2 kΩ junction at 0.5 V bias, the fractional conductance fluctuation is then

$$\Delta G/G_s = \Delta I/I_b = 4 \times 10^{-6}.$$

This is a factor 4000 larger than the minimum estimate (13) from experiment, so from section 6.6, the number of fluctuators required to give the maximum measured noise is $2 \times 10^{10}/(4000)^2 \simeq 1000$, which is reasonable for the junction area 10^{-8} m^2.

6.9. Bias dependence

The switching of resonant tunnelling channels generates current noise i_n which is related to the conductance noise g_n and measured voltage noise v_n by

$$i_n/I_b = g_n/G_s = v_n/Z_s I_b$$

(from (1)). Using (11), the current noise power is

$$i_n^2 = N_a(V)(\Delta I)^2/[4f\ln(\tau_{max}/\tau_{min})]$$

so the bias dependence of i_n is determined by

$$i_n \propto \sqrt{N_a}\Delta I.$$

Figure 10 is a log–log plot of the current noise data shown earlier in figure 4(*a*). The gradient of a linear fit decreases from 2.7 to 2.0 with increasing frequency, so

$$i_n \propto V^m \qquad \text{with } 2.0 < m < 2.7.$$

Possible reasons for this strong bias dependence are now discussed briefly.

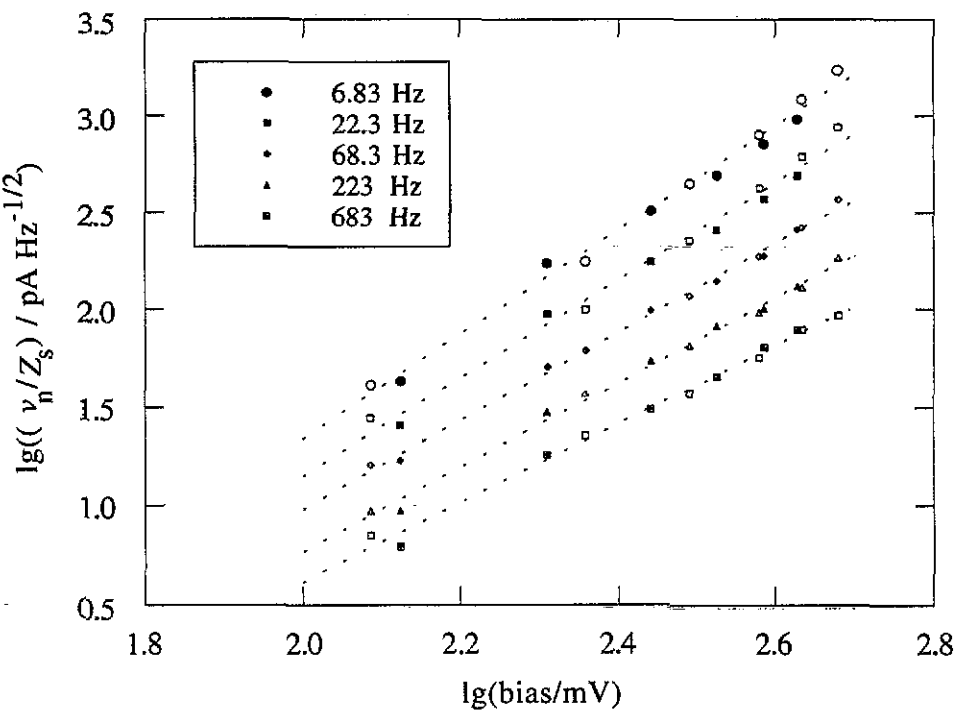

Figure 10. Log–log plot to show the bias dependence of the current noise. Open symbols show results with negative bias and filled symbols results with positive bias.

The number of active fluctuators N_a increases with bias for two reasons:

(i) a fluctuator can be switched on and off by tunnelling electrons only when the ionic excitation energy is less than the bias energy: $0 < E_i < eV$;

(*ii*) a resonant state carries a current only when the resonance energy E_{res} is within the energy range of tunnelling electrons, $0 < E_{res} < eV/2$ (for a state in the middle of the barrier) (figure 9).

If E_i and E_{res} are both uniformly distributed, each distribution introduces a factor V in the expression for N_a, so that $N_a \propto V^2$ and this contributes a factor of V in i_n.

The fluctuation size ΔI may also increase with bias, for reasons associated with the changing barrier shape. ΔI is largest for states coupled equally to both electrodes ($\Gamma_L = \Gamma_R$). As the potential across the junction is increased, the region containing the states which contribute most strongly to the noise moves nearer to the negative electrode. Since the tunnelling rate varies exponentially with tunnelling distance, this gives rise to an increase of ΔI with bias. This will further strengthen the voltage dependence of the noise.

Further contributions to the voltage dependence of the noise could come from non-uniform distributions of the energies E_i and E_{res}. At present we do not feel able to attempt a detailed analysis of how the noise depends on bias.

7. Summary

Noise measurements on tunnel junctions are a useful probe of the properties of the barrier material, and provide additional information not accessible from the usual conductance versus bias characterization or from inelastic electron tunnelling spectra. The results we have presented show that alumina tunnelling barriers grown under wet conditions have low frequency fluctuators which are activated by the tunnelling current when the junctions are under bias. We have argued that in these tunnelling structures the noise cannot originate in processes involving electron trapping because lifetimes could not be sufficiently long. Instead, we propose that there are ions within the barrier which move between neighbouring potential minima when excited by tunnelling electrons and that their motion gives rise to the noise. However, the noise is too large to be explained in terms of modulation of the barrier height by changes of potential associated with the ionic movement. We put forward a new model for noise generation in which ionic motion causes fluctuation of the tunnelling conductance by opening and closing resonant tunnelling channels. The analysis shows that such a mechanism does provide a satisfactory explanation for the noise observed in our experiments.

Acknowledgment

We should like to express our thanks to the Science and Engineering Research Council for a Studentship which supported one of us (AMS) during the course of this work.

References

Bowser W M and Weinberg W H 1977 *Surf. Sci.* **64** 377
Brinkman W F, Dynes R C and Rowell J M 1970 *J. Appl. Phys.* **41** 1915
Dragoset R A, Phillips E S and Coleman R V 1982 *Phys. Rev.* B **26** 5333
Dutta P and Horn P M 1981 *Rev. Mod. Phys.* **53** 497
Farmer K R, Rogers C T and Buhrman R A 1987 *Phys. Rev. Lett.* **58** 2255
Konkin M K and Adler J G 1980 *J. Appl. Phys.* **51** 5450
Kozub V I 1984 *Sov. Phys.-JETP* **59** 1303

Payne M C 1986 *J. Phys. C: Solid State Phys.* **19** 1145
Phillips W A 1981 *Phil. Mag.* B **43** 747
—— 1987 *Rep. Prog. Phys.* **50** 1657
Rogers C T and Buhrman R A 1984 *Phys. Rev. Lett.* **53** 1272
—— 1985 *IEEE Trans. Magn.* **MAG-21** 126
Savo B, Wellstood F C and Clarke J 1987 *Appl. Phys. Lett.* **50** 1757
Schäfer J and Adkins C J 1991 *J. Phys.: Condens. Matter* **3** 2907
Sleigh A K, Taylor M E, Adkins C J and Phillips W A 1989 *J. Phys.: Condens. Matter* **1** 1107
Speakman A M 1991 *PhD Thesis* Cambridge University
Van der Ziel A 1986 *Noise in Solid State Devices and Circuits* (New York: Wiley)
Wolf E L 1985 *Principles of Electron Tunnelling Spectroscopy* (Oxford: Oxford University Press)